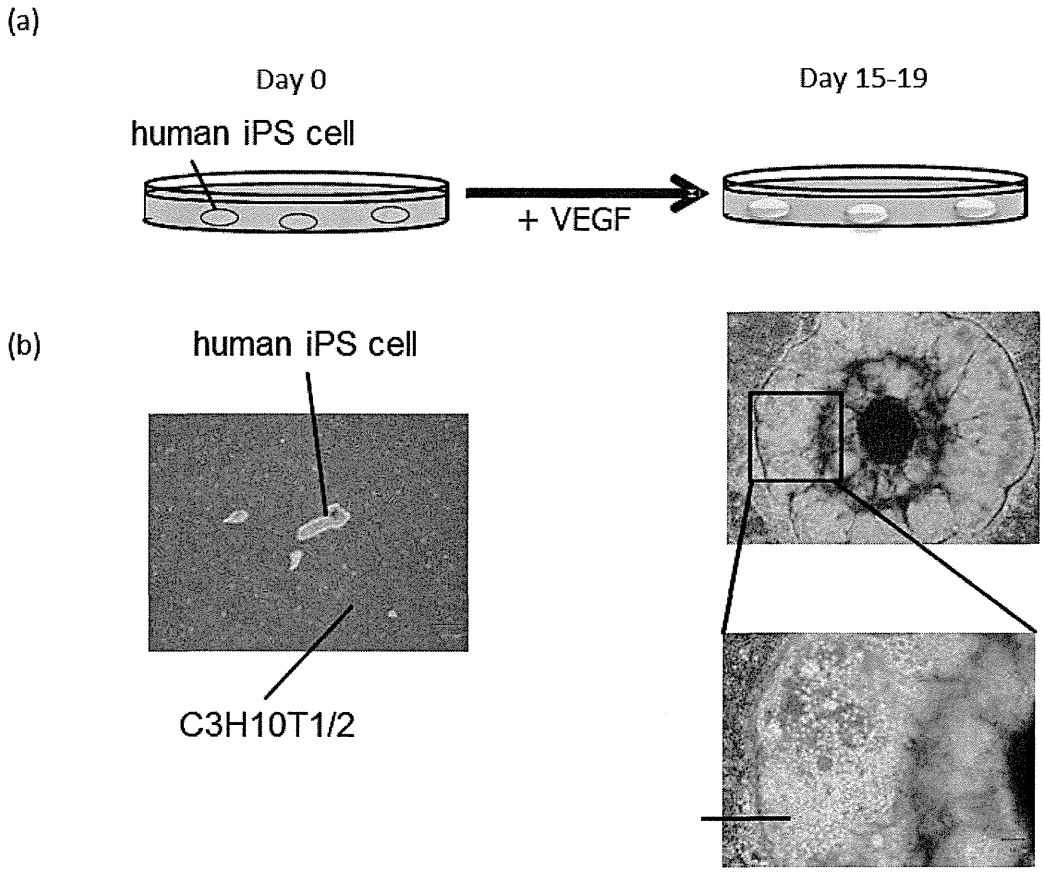

Figure 2 Human iPS cell (iPSC)-derived sac-like structure.

(a) Experimental protocol. (b) Morphology of differentiated stages on C3H10T1/2 cells (days 0 and 16).

(a)

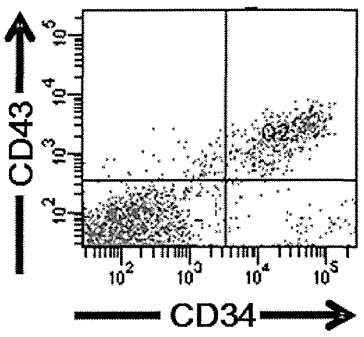

(b)

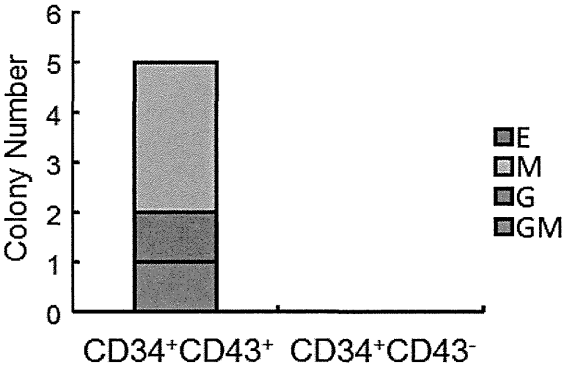

Figure 3 Hematopoietic progenitor differentiation of human iPSCs by co-culture method.

(a) Flow cytemetric analysis of human iPSC-derived cells on day 16. (b) Sorted $CD34^{+}CD43^{+}$ cells or $CD34^{+}CD43^{-}$ cells were subjected to CFU-C assay. E, M, G, and GM stand for colony containing erythroid cells, monocytes, granulocytes, and granulocytes and monocytes, respectively.

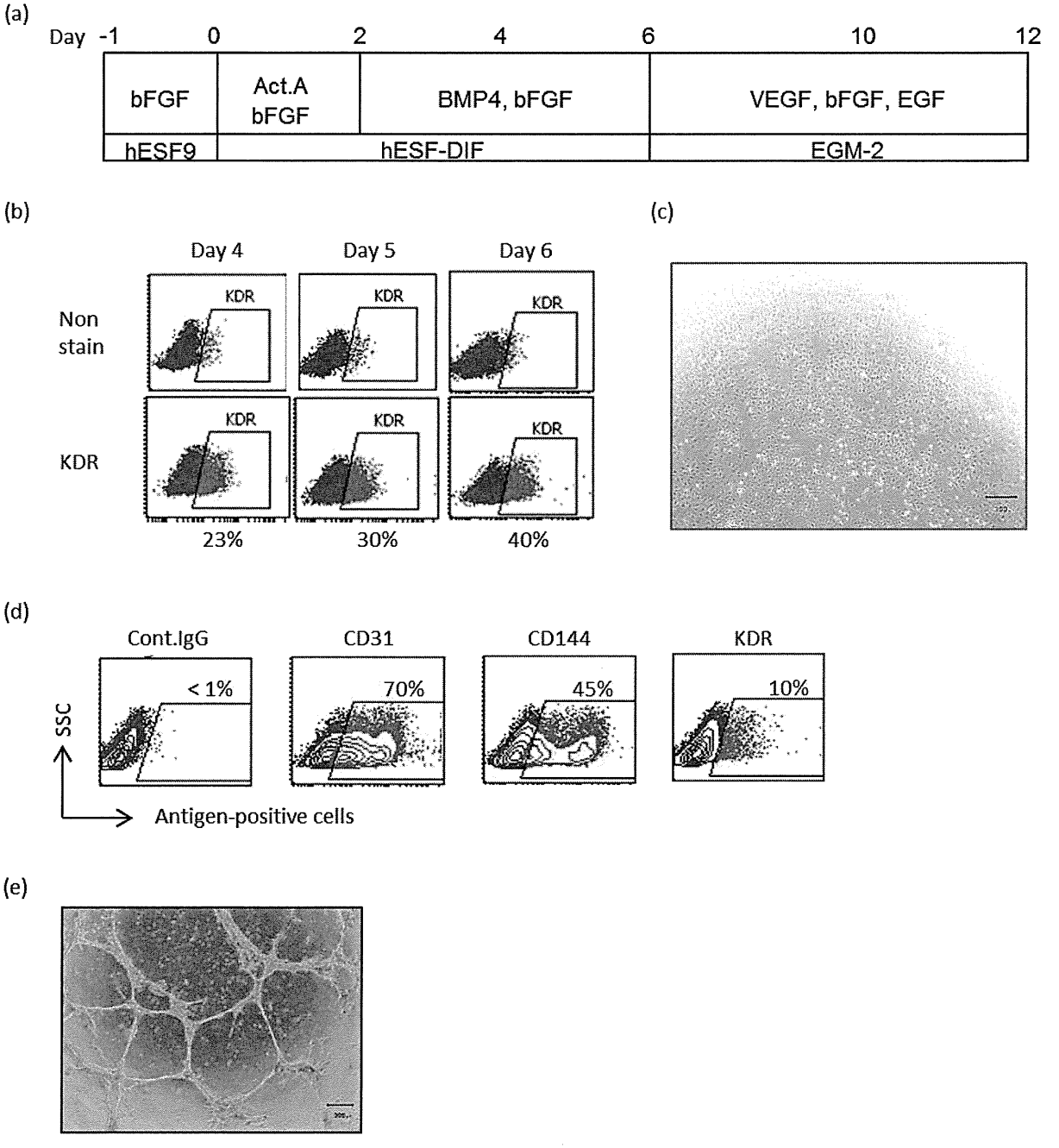

Figure 4 Endothelial differentiation of human iPSCs by monolayer culture.

(a) Experimental protocol. (b) KDR-expressing cells in human iPSC (Tic)-derived cells were analyzed by flow cytometry. (c) Morphology of iPS cell-derived cells on day 8. Scale bar indicates 300 μm. (d) Flow cytemetric analysis of human iPSC (Tic)-derived cells on day 12. (e) Tic-derived cells onto Matrigel led to vascular tube formation. Scale bar indicates 100 μm.

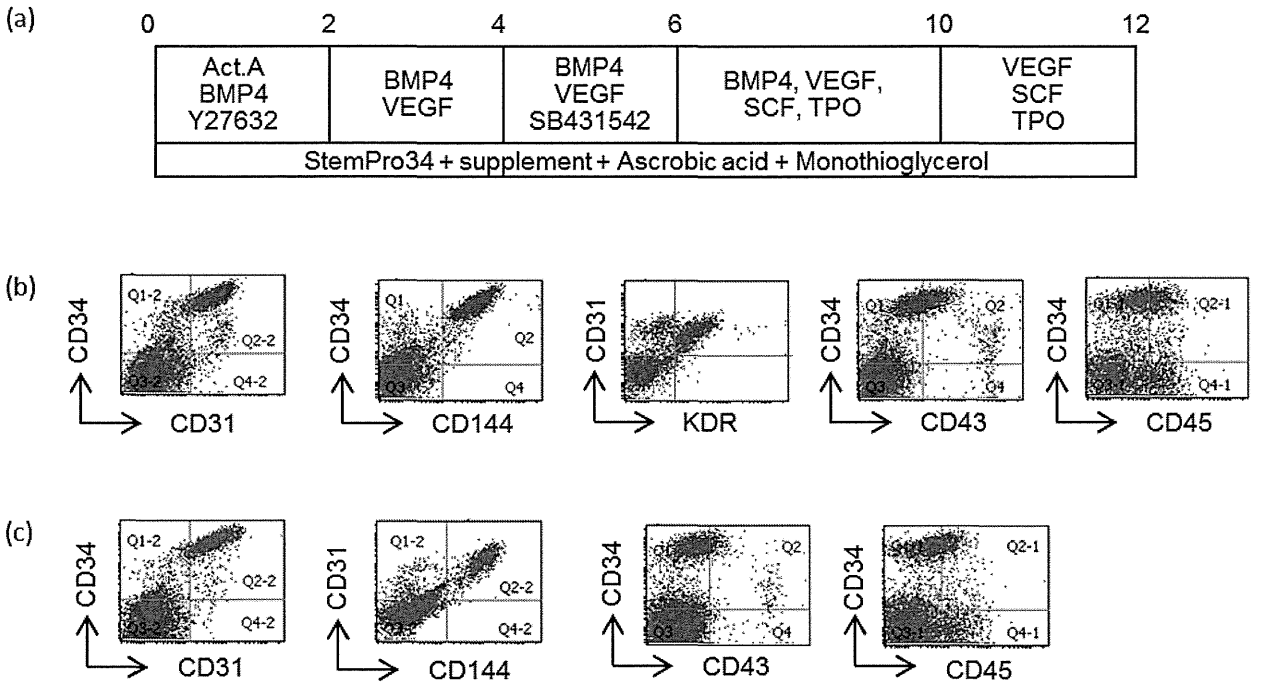

Figure 5 Endothelial differentiation of human iPSCs by EB formation.

(a) Experimental protocol. (b, c) Flow cytometric analaysis of Tic (b)- or 201B7 (c)-derived cells on day 8.

厚生労働科学研究費補助金(再生医療実用化研究事業)

分担研究報告書

ヒト iPS 細胞由来血管内皮細胞および神経細胞を用いた in vitro 血液脳関門モデルの開発および脳内移行性を包括した神経毒性評価系の構築

分担研究者　関野　祐子
国立医薬品食品衛生研究所　薬理部長

本研究では、ヒト iPS 細胞由来細胞を用いた脳内移行性を包括した神経毒性評価系の構築を目指している。今年度はヒト iPS 細胞由来神経細胞を用いた in vitro 毒性評価系の確立および従来の in vitro 血液脳関門（BBB）モデルの改良を行った。in vitro 毒性評価系としては神経細胞死評価法、シナプス機能障害評価法を確立した。また、 従来の in vitro BBB モデルにミクログリアを添加することにより、BBB バリア機能の亢進を達成した。

研究協力者
国立医薬品食品衛生研究所薬理部
佐藤　薫
最上　由香里
千川　和枝

A. 研究目的

薬物の中枢神経への作用を考えるうえでは、血液脳関門（blood brain barrier: BBB）と神経細胞、グリア細胞をユニットとしてとらえる必要があり（Fig. 1A）、脳毛細血管、ペリサイト、アストサイト、マイクログリア、神経細胞など、関連する細胞成分を包括するオールインワン型のモデルが必要である。さらに、このオールインワン型モデルをヒト細胞に置き換え、脳内移行性を考慮した in vitro 神経毒性評価系を構築することで、in vitro 実験系における薬物の有効濃度、毒性濃度のヒト予測性が向上することが期待される。本研究では、ヒト細胞として　ヒト人工多能性幹（induced pluripotent stem: iPS）細胞由来分化細胞の実用を試みる。本年度はまず、オールインワン型モデルへの組み込みに適した、ヒト iPS 細胞由来神経細胞による in vitro 神経毒性評価系を確立する。並行して、内皮細胞、ペリサイト、アストロサイトにより構成される従来の in vitro BBB モデルにその他の中枢神経系細胞成分（ミクログリアなど）を添加することにより BBB モデルの改良をラット由来細胞を用いて試みる。これらを組み合わせることにより、ヒト iPS 細胞由来細胞を用いた脳内移行性を包括した神経毒性評価系の構築が可能となる（Fig. 1B）。

B. 研究方法

1. ヒト iPS 細胞由来神経細胞を用いた in vitro 毒性評価系の構築

1-1. 神経細胞死評価法の構築

ヒト iPS 細胞（253G1 株）由来神経幹細胞塊を単一細胞に分散したのち神経細胞に分化誘導し、分化誘導 20 日目に propidium iodide (PI) (2 μM) および Hoechst 33342 (1 μg/ml) を培地に添加した。24 時間後、細胞を共焦点レーザー顕微鏡（Nikon A1）により観察した。

1-2. シナプス機能障害評価法の構築

マウス 胚性幹 (embryonic stem: ES) 細胞から胚様体形成を介して神経幹細胞塊を得た。神経幹細胞塊を単一細胞に分散したのち神経細胞に分化誘導し、分化誘導 14 日目に fura2-AM をとりこませ、AQUACOSMOS システム (Hamamatsu photonics) を用いて各種リガンドによって引き起こされる細胞内カルシウム変動を可視化した。特に、シナプスを介した神経回路機能を反映する自発的な発火や 抑制性神経伝達物質である gamma aminobutylic acid (GABA) 受容体の阻害薬ピクロトキシン（50 μM, 2min 適用）への反応に注目した。同様のプロトコルでヒト iPS 細胞 (253G1) 由来神経細胞についても検討した。

2. in vitro 血液脳関門（BBB）モデルの改良

市販の In vitro BBB モデル（内皮細胞、ペリサイト、アストロサイトより構成されている）を解凍し、初代培養ミクログリアを 6 x 10^4 cells/cm^2 の細胞密度で脳側チャンバーのアストロサイト上に添加した。BBB 機能成熟期間（5 日間）インキュベートした後、内皮抵抗値（TEER）を測定し、ミクログリア非添加群と比較することにより、BBB のバリア機能への影響を検討した。

C. 研究結果

1. ヒト iPS 細胞由来神経細胞を用いた in vitro 毒性評価系の構築

1-1. 神経細胞死評価法の構築

我々はすでにヒト iPS 細胞（253G1 株）由来神経幹細胞から神経細胞を分化誘導する際、20 日目から生存細胞数の急激な減少が起こることを見いだしていた。そこで、この条件下で生細胞と死細胞の可視化を試みた（Fig. 2A）。Hoechst 染色により全細胞（生細胞および死細胞の両者）の核が可視化され、PI は細胞膜に侵襲のある細胞にとりこまれ、死細胞の核を可視化した。すでにヒト iPS 細胞由来神経幹細胞から我々の採用した分化プロトコルにより誘導される細胞はほぼ 100 % 神経細胞であることを確認している。従って、以下のクライテリアにより定量的な神経細胞死評価が可能になった。

生細胞：Hoechst 染色により核が明確に判別できる。PI 蛍光が見られない。

死細胞：Hoechst 染色は陽性であるが、核の輪郭ははっきりしない。PI 蛍光が核に集積している。

また、PI 染色像によりアポトーシスの特徴とされる DNA 断片化やアポトーシス小体も明確に判別できることがわかった（Fig. 2A, arrowheads）。

1-2. シナプス機能障害評価法の構築

マウス ES 細胞から分化誘導した神経細胞は分化誘導 14 日目で自発的なカルシウム振動が現れた（Fig. 2B, b1, arrowheads）。このカルシウム振動は Na^+ チャネル阻害剤である tetrodotoxin (TTX) によって消失したことから（データ示さず）、神経細胞の自発的な発火によるものであることが示された。また、GABA 受容体阻害

薬であるピクロトキシンを適用すると、この振動の振幅と頻度がともに増大した。GABA 受容体阻害薬によりカルシウム振動が増大したことは、抑制性の入力が阻害されて興奮性神経回路が活性化したことを示しており、この標本において興奮性および抑制性の神経回路が形成され神経細胞の自発的な発火が起こっていることを示している。同様の実験を 253G1 由来神経細胞についても検討したが、現在のところ、自発発火は観察されていない。また、ピクロトキシンを適用しても細胞内カルシウムに変動は起こらなかった。

その他、細胞骨格タンパク質であるドレブリンをバイオマーカーとしてシナプス機能への影響を評価する手法を立ち上げている（Fig. 2B, b2）。本実験系についてはすでに培養技術、ドレブリン染色法の導入をすませており、現在、定量プロトコルを確立中である。

2. in vitro 血液脳関門（BBB）モデルの改良

ミクログリア を従来型 BBB モデルに添加すると、 TEER の有意な上昇が起こった（Fig. 3）。上昇率はコントロールの 1.46 倍であった。これは、ミクログリアにより BBB のバリア機能形成が促進したことを反映していると考えられる。

D. 考察

1. ヒト iPS 細胞由来神経細胞を用いた in vitro 毒性評価系の構築

1-1. 神経細胞死評価法の構築

今年度の研究成果としてヒト iPS 細胞由来神経細胞の生細胞と死細胞の可視化、および定量化を達成した。PI は DNA の二重らせん構造に intercalate することにより特有の赤色蛍光（620 nm）が増強される。生細胞と死細胞が共存している条件では、細胞膜が侵襲をうけている死細胞のみにとりこまれ、蛍光を発することから、これまでフローサイトメトリーなどへ応用されていたが、今回、ヒト iPS 細胞由来神経細胞の神経細胞死評価にも有効であることが示された。ただし、PI は二本鎖構造の核酸と intercalate して赤色蛍光を発するため、二本鎖 RNA と結合してもわずかに蛍光を発する。従って、正確な定量を行うためには、核以外の蛍光レベルをほぼ 0 にするよう、検出機器のブラックレベルを調整する必要があるであろう。また、PI 染色ではアポトーシスを起こした細胞の DNA 断片化やアポトーシス小体も明確に判別できた。従って死細胞数の定量的な情報に加えて定性的な情報（細胞死がアポトーシスによるものか、ネクローシスによるものか、等）も得ることが可能そうである。

1-2. シナプス機能障害評価法の構築

カルシウムイメージング手法を応用し、シナプスを介した神経回路機能に対する障害の定量法を確立した。マウス ES 細胞由来神経細胞標本では分化誘導 14 日目に神経細胞の自発的な発火が観察された。さらに抑制性入力の阻害により、興奮性神経回路機能の増強が確認された。こうしたシナプスを介した神経回路機能に由来するカルシウム応答に対する薬物の作用を定量化することにより、シナプス機能障害評価が可能となる。253G1 由来神経細胞について同様の検討を行ったが、現在のところ自発発火は観察されていない。しかし、253G1 由来神経細胞の生存や分化を促進する条件をすでに複数発見しており、今後この条件での検討を進める予定である。現在、カルシウムイメージング以外にも細胞骨格タンパク質ドレブリンをバイオマーカーとしてシナプス機能への影響を評価する手法を立ち上げている。アクチン結合蛋白質であるドレブリンはシナプス機能が正常な時は、後シナプス部位であるスパインに集積しているが、シナプス機能に異常が現れると局在が樹状突起に分散する。従って、ドレブリンのスパイン集積度をシナプス機能障害のパラメーターとして応用することができる。

2. in vitro 血液脳関門（BBB）モデルの改良

ミクログリアは有意に BBB のバリア機能形成を促進させた。分子レベルでの詳細な解析は今後進める予定であるが、我々は生後初期の神経新生、グリア新生をミクログリアが複数のサイトカインを介して促進することを見いだしている（投稿中）。従って、同様のメカニズムにより、内皮細胞の機能分化を促進している可能性も考えられる。我々が構築しているモデル系は従来のモデル系より生体内の脳に近いことから、薬物や障害に対する反応性に関してこれまでのモデルとの比較データをとる必要があろう。また、実際薬物を服用するのは炎症等の症状がすでに現れた患者であることを鑑みると、病態時の BBB がどのような状態であるのか、という点についても検討の必要がある。そこで、炎症誘発モデルとして汎用されている lipopolysaccharide 適用に対する BBB バリア機能の変化についても我々のモデルと従来のモデルとの比

較検討を現在行っている。

E. 結論

ヒト iPS 細胞由来神経細胞を用いた in vitro 毒性評価系として、神経細胞死評価法、シナプス機能障害評価法を確立した。また、従来の in vitro BBB モデルにミクログリアを添加することにより、BBB バリア機能の亢進を達成した。

F. 研究発表

1. 論文発表　（＿は研究協力者）

1) Shigemoto-Mogami, Y., Goldman, J.E., Sekino, Y., Sato, K., Microglia enhance neurogenesis and oligodendrogenesis in the early postnatal subventricular zone (submitted)
2) ,Oguchi-Katayama, A., Monma, A., Sekino, Y., Moriguchi, T, Sato, K. Comparative gene expression analysis of the amygdalae of juvenile rats exposed to valproic acid at prenatal and postnatal stages. (in revision)
3) Takaki, J., Fujimori, K., Miura M., Suzuki T., Sekino, Y., Sato, K., L-glutamate released from activated microglia downregulates astrocytic L-glutamate transporter expression in neuroinflammation: the 'collusion' hypothesis for increased extracellular L-glutamate concentration in neuroinflammation. ***J. Neuroinflammation***, 9, 275 (2012)
4) Sato, K., Kuriwaki J., Takahashi, K., Saito, Y., Oka, J., Otani, Y., Sha, Y., Nakazawa, K., Sekino, Y., Ohwada, T. Discovery of a tamoxifen-related compound that suppresses glial L-glutamate transport activity without Interaction with estrogen receptors. ***ACS Chem Neurosci***, 3 (2), 105-113 (2012)

2. 学会発表

＜国内学会＞

1. 最上（重本）由香里、　千川和枝、三浦麻利衣、関野祐子、佐藤　薫、神経細胞とグリア細胞（アストロサイト・ミクログリア）が共存する新規 In Vitro 血液脳関門モデルの開発、日本薬学会第 133 回年会（2013.3）（横浜）
2. 高橋華奈子、最上（重本）由香里、大津香苗、岡田洋平、岡野栄之、関野祐子、佐藤薫、ヒト iPS 細胞由来神経細胞標本の遺伝子発現プロファイリングの株間比較、日本薬学会第 133 回年会（2013.3）（横浜）
3. 片山敦子、門馬彰彦、秋友孝文、廣末　愛、星裕姫乃、守口　徹、関野祐子、佐藤　薫、バルプロ酸幼弱期暴露が情緒社会性におよぼす影響を予測するマーカー遺伝子群の探索、日本薬学会第 133 回年会（2013.3）（横浜）
4. 佐藤　薫、片山敦子、門馬彰彦、守口　徹、関野祐子、バルプロ酸を胎生期あるいは生後適用したラット扁桃体の遺伝子発現マイクロアレイ解析、第 86 回　日本薬理学会年会（2013.3）（福岡）
5. 最上由香里、大野泰雄、ジェームズ E ゴールドマン、関野祐子、佐藤　薫、ミクログリアは生後初期脳室下帯の神経新生、オリゴデンドロサイト新生を促進する、第 86 回　日本薬理学会年会（2013.3）（福岡）
6. 大和田智彦、佐藤　薫、栗脇淳一、高橋華奈子、斉藤善彦、岡　淳一郎、中澤憲一、関野祐子、沙宇、尾谷優子、タモキシフェンを基盤としたグルタミン酸トランスポーター阻害剤の開発、第 30 回　メディシナルケミストリーシンポジウム（2012. 11）（東京）
11. Shigemoto-Mogami, Y., Fujimori, K., Igarashi, Y., Hirose, A., Sekino Y., Sato, K., Effects of carbon nanotubes on proliferation of neural stem cells and microglial viability, 第 35 回　日本神経科学大会（2012. 9）（名古屋市）
12. Takahashi, K., Tomohiko I., Sekino, Y., Sato, K., Development of the epitope-tagged EAAT2 in Xenopus oocyte expression system, 第 35 回　日本神経科学大会（2012. 9）（名古屋市）
13. Oguchi-Katayama, A., Monma, A., Otomo, Y., Imai, M., Akitomo, T., Takahashi, Y., Kato, F., Sekino, Y.,

Sato, K., Search for genetic markers for risks in emotion and social interaction caused by exposure to chemical compounds in embryonic or neonatal periods, 第35回　日本神経科学大会（2012. 9）（名古屋市）

14. Sato, K., Takahashi, K., Shigemoto-Mogami, Y., Ohtsu, K., Okada, Y., Okano, H., Sekino, Y., The Clonal difference in response to L-glutamate and ATP of human induced pluripotent stem cell-derived neurons, 第 35 回　日本神経科学大会（2012. 9）（名古屋市）
15. 最上(重本)由香里、関野祐子、佐藤　薫、生後ラットの脳・SVZ 周辺において活性化ミクログリアは神経およびグリア細胞の新生・分化を制御している、第 14 回応用薬理研究会（2012. 9, 甲府市）
16. 片山　敦子、守口　徹、関野祐子、佐藤薫、幼弱期化学物質暴露による情緒社会性への影響の予測、第 14 回応用薬理研究会（2012. 9）（甲府市）
17. 高橋華奈子、入江智彦、関野祐子、佐藤 薫、グルタミン酸トランスポーター EAAT2 機能調節機構の解析ツールとしてのエピトープ標識 EAAT2 の開発、第 14 回応用薬理研究会（2012. 9, 甲府市）
18. 佐藤　薫、栗脇淳一、高橋華奈子、齊藤善彦、岡　淳一郎、尾谷祐子、謝宇、中澤憲一、関野祐子、大和田智彦、 タモキシフェンを基盤とした新規グルタミン酸トランスポーター阻害剤の開発、第 14 回応用薬理研究会（2012. 9）（甲府市）

＜国際学会＞

1. Sato, K., Fujimori, K., Takaki, J., Suzuki, T., Sekino, Y., Paroxetine Prevents the Functional Impairment of L-Glutamate Transporters in Inflammation by Modulating Microglial Glutamate Release. SfN 2012 (2012. 10) (New Orleans, USA)
2. Sato, K., Takahashi, K., Shigemoto-Mogami, Y., Ohtsu, K., Okada, Y., Okano, Y., Sekino, Y., The comparative study of the mRNA-expression of P2 receptors and glutamate receptors between neurons differentiated from 201B7 and 253G1 human induced pluripotent stem cell lines. the 11th biennial meeting of APSN and the 55th annual meeting of JSN (2012. 9) (Kobe, Japan)
3. Sekino, Y., Takahashi, K., Shigemoto-Mogami, Y., Ohtsu, K., Okada, Y., Okano, Y., Sato, K., The clonal difference in response to ATP and L-Glutamate of human induced pluripotent stem cell-derived neurons, the 11th biennial meeting of APSN and the 55th annual meeting of JSN (2012. 9) (Kobe, Japan)
4. Sato, K., Kuriwaki, J., Takahashi, K., Saito, Y., Oka, J., Otani, Y., Sha, Y., Nakazawa K., Sekino, Y., Ohwada, T. Discovery of a tamoxifen-related compound that suppresses glial L-glutamate transport activity without interaction with estrogen receptors, FENS meeting 2012 (2012.7) (Barcelona, Spain)
6. Sato, K., Takahashi, K., Shigemoto-Mogami, Y., Ohtsu, K., Okada, Y., Okano, H., Sekino, Y. The clonal difference in response to ATP of human induced pluripotent stem cell-derived neurons, ISSCR2012 (2012.6), (Yokohama, Japan)
7. Sato, K., Takahashi, K., Shigemoto-Mogami, Y., Ohtsu, K., Okada, Y., Okano, H., Sekino, Y. The clonal difference in response to ATP of human induced pluripotent stem cell-derived neurons, Purine2012 (2012.5-6), (Fukuoka, Japan).

G. 知的財産権の出願・登録状況

1. 特許取得

なし

2. 実用新案登録

なし

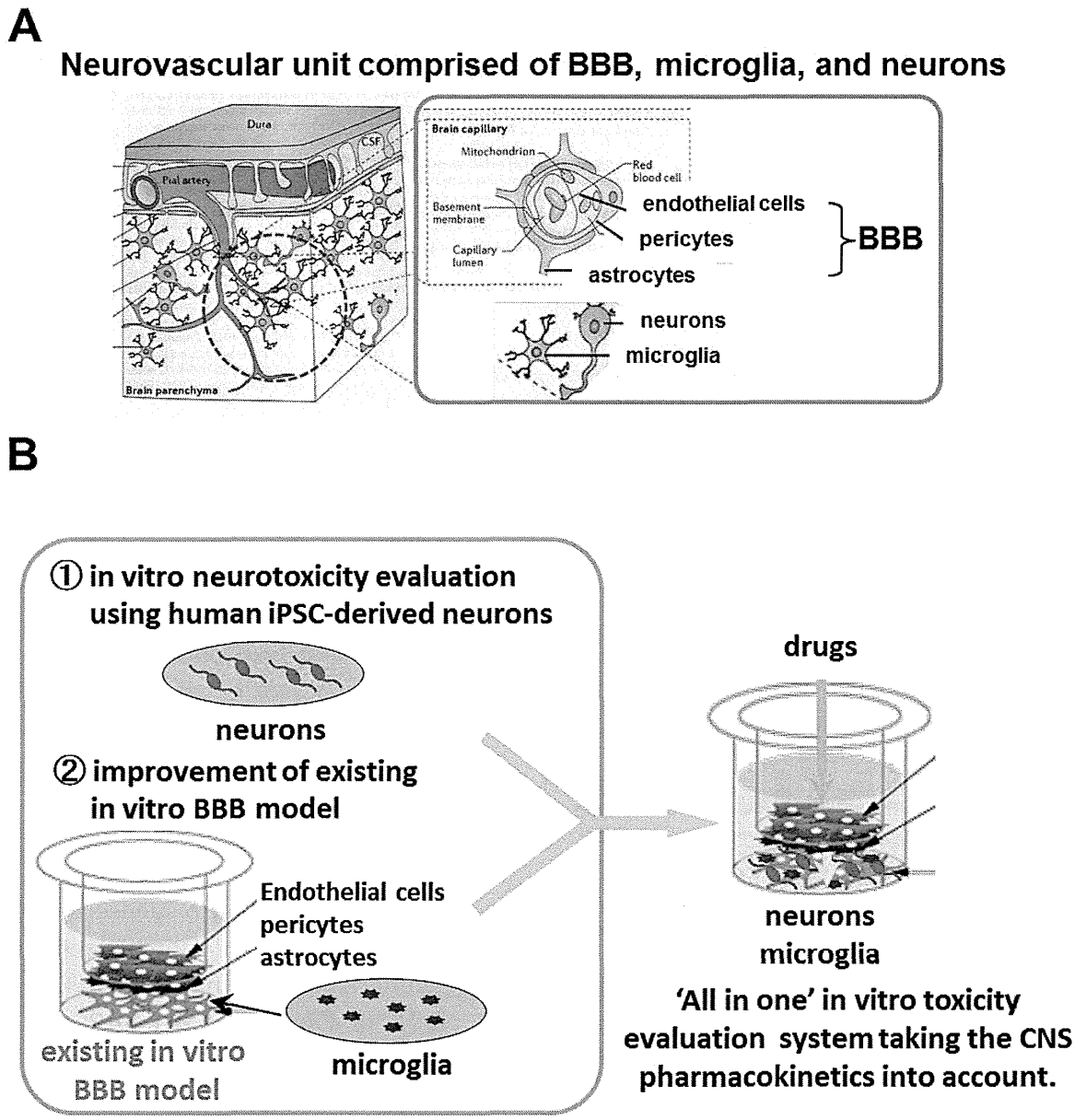

Fig. 1 The concept for the 'All in one' in vitro toxicity evaluation system

(A) Neurovascular unit (NVU) is comprised of the blood-brain barrier (BBB), microglia, and neurons. Because drugs in the central nervous system (CNS) reach neurons via BBB, the model system reproducing NVU is necessary to predict adverse effects on the CNS functions. (B) the experimental plan in this year. ① The developing in-vitro neurotoxicity evaluation sustem using iPSC-derived neurons. ② The existing in vitro BBB model is comprised of endothelial cells, pericytes and astrocytes. We will establish the 'all in one' in vitro toxicity evaluation system taking the CNS pharmacokinetics into account.

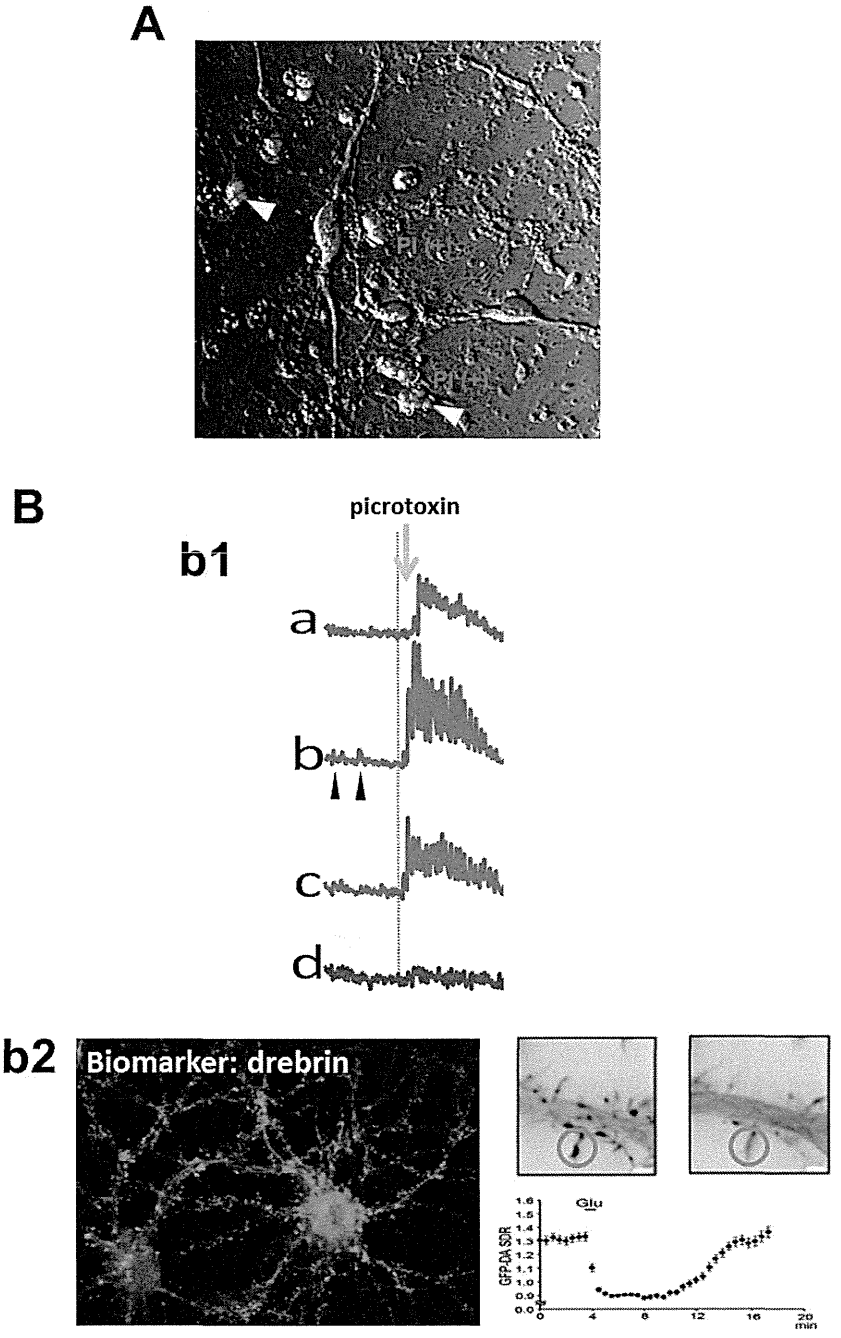

Fig. 2 In vitro toxicity evaluation system using human iPS cell-derived neurons.

(A) Establishment of evaluation method for neuronal death. human iPS-derived neurons (253G1) were double-stained with Hoechst 33342 and PI. This method allowed to discriminate dead cells from viable cells. Apoptotic cells could be also determined by DNA fragmentation and apoptotic bodies revealed by PI staining (arrowheads). (B) Establishment of the evaluation methods for impaired synaptic function. b1: typical traces of $[Ca^{2+}]_{in}$ of the mouse ES-derived neurons loaded with fura2-AM after 14 d-differentiation period. Spontaneous $[Ca^{2+}]_{in}$ increase was observed and Picrotoxin (50 mM, 2 min) increased the amplitude and frequency of the responses. b2: typical image of the immunostained drebrin in cultured rat neurons (left). The localization of drebrin was changed by the stimulation with L-glutamate.

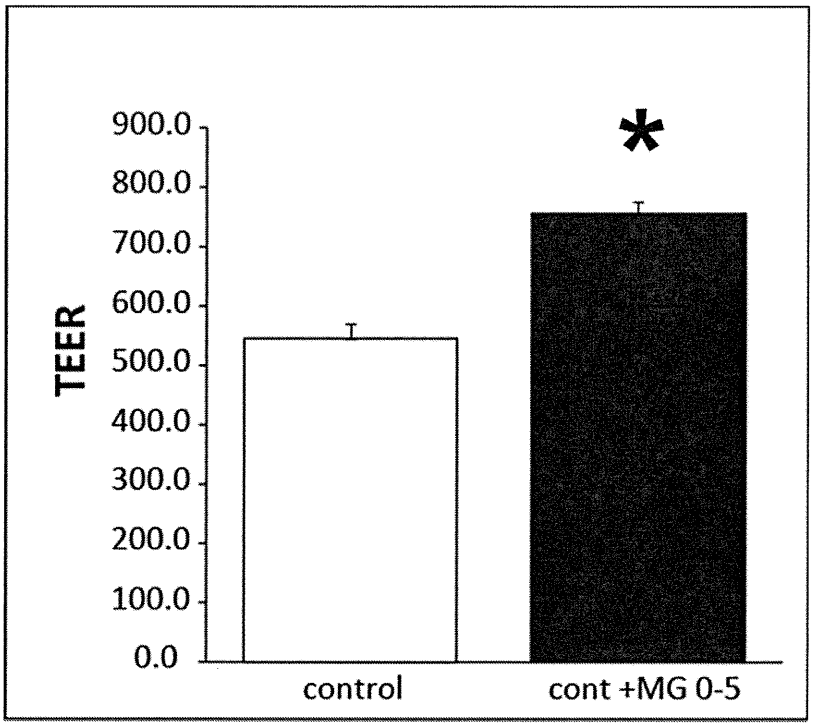

Fig. 3 Supplement of in vitro BBB model with microglia significantly increased the TEER

Primarily-cultured microglia were added on the astrocytes in the existing BBB kit. After 5 d-maturation period, TEER of the BBB was measured using Endohm with EVOM2. Microglia significantly increased the TEER. (*: $P<0.05$ vs. control group. student's *t* test, N=4.)

別紙４

研究成果の刊行に関する一覧表

書籍

著者氏名	論文タイトル名	書籍全体の編集者名	書　籍　名	出版社名	出版地	出版年	ページ

雑誌

発表者氏名	論文タイトル名	発表誌名	巻号	ページ	出版年
Yamaguchi T., Tashiro K., Tanaka S., Katayama S., Ishida W., Fukuda K., Fukushima A., Araki R., Abe M., Mizuguchi H., **Kawabata K.**	Two-step differentiation of mast cells from induced pluripotent stem cells.	***Stem Cells Dev.***	22	726-734	2013
Tashiro K., Omori M., **Kawabata K.**, Hirata N., Yamaguchi T., Sakurai F., Takaki S., Mizuguchi H.	Inhibition of Lnk in Mouse Induced Pluripotent Stem Cells Promotes Hematopoietic Cell Generation.	***Stem Cells Dev.***	21	3381-3390	2012
Tashiro K., **Kawabata K.**, Omori M., Yamaguchi T., Sakurai F., Katayama K., Hayakawa H., Mizuguchi H.	Promotion of hematopoietic differentiation from mouse induced pluripotent stem cells by transient HoxB4 transduction.	***Stem Cell Res.***	8	300-311	2012
Takayama K., **Kawabata K.**, Nagamoto Y., Kishimoto K., Tashiro K., Sakurai F., Tachibana M., Kanda K., Hayakawa T., Furue MK., Mizuguchi H.	3D spheroid culture of hESC/hiPSC-derived hepatocyte-like cells for drug toxicity testing.	***Biomaterials***	34	1781-1789	2013

Takayama K., Inamura M., **Kawabata K.**, Sugawara M., Kikuchi K., Higuchi M., Nagamoto Y., Watanabe H., Tashiro K., Sakurai F., Hayakawa T., Furue MK., Mizuguchi H.	Generation of metabolically functioning hepatocytes from human pluripotent stem cells by FOXA2 and HNF1α transduction.	***J. Hepatol.***	57	628-636	2012
Nagamoto Y., Tashiro K., Takayama K., Ohashi K., **Kawabata K.**, Sakurai F., Tachibana M., Hayakawa T., Furue MK., Mizuguchi H.	The promotion of hepatic maturation of human pluripotent stem cells in 3D co-culture using type I collagen and Swiss 3T3 cell sheets.	***Biomaterials***	33	4526-4534	2012
Takayama K., Inamura M., **Kawabata K.**, Katayama K., Higuchi M., Tashiro K., Nonaka A., Sakurai F., Hayakawa T., Furue MK., Mizuguchi H.	Efficient generation of functional hepatocytes from human embryonic stem cells and induced pluripotent stem cells by HNF4α transduction.	***Mol. Ther.***	20	127-137	2012
Takaki J., Fujimori K., Miura M., Suzuki T., **Sekino, Y.**, Sato, K.	L-glutamate released from activated microglia downregulates astrocytic L-glutamate transporter expression in neuroinflammation: the 'collusion' hypothesis for increased extracellular L-glutamate concentration in neuroinflammation.	***J. Neuro-inflammation***	9	275	2012
Sato K., Kuriwaki J., Takahashi K., Saito Y., Oka J., Otani Y., Sha Y., Nakazawa K., **Sekino Y.**, Ohwada T.	Discovery of a tamoxifen-related compound that suppresses glial L-glutamate transport activity without Interaction with estrogen receptors.	***ACS Chem Neurosci***	3 (2)	105-113	2012
Kawabata K., Takayama K., Nagamoto Y., Saldon MM., Higuchi M., Mizuguchi H.	Endodermal and hepatic differentiation from human embryonic stem cells and human induced pluripotent stem cells.	***J. Stem Cell Res. Ther.***	S10	002	2012
Kawabata K., Inamura M., Mizuguchi H.	Efficient hepatic differentiation from human iPS cells by gene transfer.	***Methods Mol. Biol.***	826	115-124	2012

水口裕之、高山和雄、長基康人、**川端健二**	ヒトiPS細胞から肝細胞への分化誘導の現状と創薬応用	医薬品医療機器レギュラトリーサイエンス	43	982-987	2012
高山和雄、**川端健二**、水口裕之	ヒトES/iPS細胞から肝細胞への高効率分化誘導法の開発とその創薬応用	最新医学	68	141-144	2013
川端健二、高山和雄、水口裕之	ヒトiPS細胞由来分化誘導肝細胞を用いた薬物毒性評価系の開発	バイオインダストリー	30	19-24	2013

SCD-2012-0339-ver9-Yamaguchi_1P
Type: research-article

STEM CELLS AND DEVELOPMENT
Volume 00, Number 00, 2012

DOI: 10.1089/scd.2012.0339

ORIGINAL RESEARCH REPORT

AU1 ▶

Two-Step Differentiation of Mast Cells from Induced Pluripotent Stem Cells

AU2 ▶ Tomoko Yamaguchi,[1] Katsuhisa Tashiro,[1] Satoshi Tanaka,[2] Sumie Katayama,[3] Waka Ishida,[4] Ken Fukuda,[4] Atsuki Fukushima,[4] Ryoko Araki,[5] Masumi Abe,[5] Hiroyuki Mizuguchi,[1,6,7] and Kenji Kawabata[1,6]

Mast cells play important roles in the pathogenesis of allergic diseases. They are generally classified into 2 phenotypically distinct populations: connective tissue-type mast cells (CTMCs) and mucosal-type mast cells (MMCs). The number of mast cells that can be obtained from tissues is limited, making it difficult to study the function of mast cells. Here, we report the generation and characterization of CTMC-like mast cells derived from mouse induced pluripotent stem (iPS) cells. iPS cell-derived mast cells (iPSMCs) were generated by the OP9 coculture method or embryoid body formation method. The number of Safranin O-positive cells, expression levels of CD81 protein and histidine decarboxylase mRNA, and protease activities were elevated in the iPSMCs differentiated by both methods as compared with those in bone marrow-derived mast cells (BMMCs). Electron microscopic analysis revealed that iPSMCs contained more granules than BMMCs. Degranulation was induced in iPSMCs after stimulation with cationic secretagogues or vancomycin. In addition, iPSMCs had the ability to respond to stimulation with the IgE/antigen complex *in vitro* and *in vivo*. Moreover, when iPSMCs generated on OP9 cells were cocultured with Swiss 3T3 fibroblasts, protease activities as maturation index were more elevated, demonstrating that mature mast cells were differentiated from iPS cells. iPSMCs can be used as an *in vitro* model of CTMCs to investigate their functions.

Introduction

MAST CELLS HAVE recently gained attention, because they have been recognized as effector cells not only in allergic disorders, but also in other immune diseases, including autoimmune diseases and chronic inflammatory disorders [1]. Activation of mast cells triggers allergic and inflammatory responses through the release of a wide variety of mediators, such as histamine, arachidonic acid metabolites, and neutral proteases, and regulates immune responses through the production of cytokines and chemokines [2]. Mast cell precursors leave the bone marrow, migrate in the blood, invade tissues, and then proliferate and differentiate into mature cells [3]. Mature rodent mast cells are generally classified into 2 phenotypically distinct populations: connective tissue-type mast cells (CTMCs) and mucosal-type mast cells (MMCs) [3–4]. Each cell type differs with respect to location, staining characteristics, and histamine content. Mouse CTMCs, which are present in the peritoneal cavity and skin, contain heparin and store large amounts of histamine. In contrast, mouse MMCs, which are prominent in the mucosal layer of the gastrointestinal tract, contain chondroitin sulfate E rather than heparin and have relatively low histamine content. Since recent studies have demonstrated that CTMCs are involved in a wide variety of immune responses [5–7], development of an *in vitro* culture system of CTMCs is needed. Although several mast cell lines and IL-3-dependent bone marrow-derived mast cells (BMMCs) have been used as models to investigate the process of mast cell activation and subsequent production of proinflammatory mediators, these models have limitations in analyzing the functions specific to mature mast cells. Previous studies showed that coculture of BMMCs with Swiss 3T3 fibroblasts in the presence of stem cell factor (SCF) facilitated morphological and functional maturation toward a CTMC-like phenotype [8].

Differentiation of both mouse and human embryonic stem (ES) cells into multiple hematopoietic lineages is now well established as a powerful tool for studying hematopoietic

[1]Laboratory of Stem Cell Regulation, National Institute of Biomedical Innovation, Osaka, Japan.
[2]Department of Immunobiology, Okayama University Graduate School of Medicine, Dentistry, and Pharmaceutical Sciences, Okayama, Japan.
[3]Bioresources Research, Laboratory of Common Apparatus, National Institute of Biomedical Innovation, Osaka, Japan.
[4]Department of Ophthalmology and Visual Science, Kochi Medical School, Kochi, Japan.
[5]Transcriptome Research Group, National Institute of Radiological Sciences, Chiba, Japan.
[6]Graduate School of Pharmaceutical Sciences, Osaka University, Osaka, Japan.
[7]The Center for Advanced Medical Engineering and Informatics, Osaka University, Osaka, Japan.

differentiation and lineage restriction, and for generating unlimited numbers of hematopoietic stem and progenitor cell populations for transplantation [9–12]. ES or induced pluripotent stem (iPS) cells into hematopoietic cells have been differentiated by embryoid body (EB) formation or coculture with stromal cells, such as OP9 cells [13–16]. By using these protocols, several groups have previously established methods to generate mast cells from mouse [17–19], cynomolgus monkey [20], and human [21] ES cells. ES cell-derived mast cells could respond to stimulation with antigen and substance P by releasing histamine. However, in most cases, these cells do not develop the large granules and high levels of proteolytic enzymes characteristic of tissue mast cells.

In this study, we generated mast cells from mouse iPS cells (iPSMCs), and characterized them from the point of view of morphology, function, and gene expression. Our results showed that the iPSMCs that were differentiated by coculture with OP9 stromal cells or the EB formation method had characteristics similar to CTMCs. When iPSMCs that were generated on OP9 cells were cocultured with Swiss 3T3 fibroblasts, the iPSMCs exhibited a more functional phenotype.

Materials and Methods

Cell cultures

Two mouse iPS cell clones, 38C2 (a kind gift from Dr. S. Yamanaka, Kyoto University, Kyoto, Japan) [22] and 2A-EGFPTg-4F-01 [23], were used in the present study. These mouse iPS cells were routinely cultured in a leukemia inhibitory factor-containing ES cell medium (Specialty Media) on mytomycin C-treated mouse embryonic fibroblasts (MEFs; Specialty Media), and they were passaged every 2 days using 0.25% trypsin-EDTA (Invitrogen). OP9 stromal cells were cultured in an α-minimum essential medium (α-MEM: Sigma) supplemented with 20% fetal bovine serum (FBS), 2 mM L-glutamine (Invitrogen), and 1×nonessential amino acid (NEAA; Invitrogen).

Generation of BMMCs

C57BL/6 mice were purchased from Nippon SLC. Bone marrow cells were prepared from the femurs and tibiae of mice. Cells were cultured in an RPMI 1640 medium containing 10% FBS, 1×NEAA, and 10 ng/mL murine IL-3 (R&D Systems). The culture medium was replaced with a fresh medium every 5 days. After 4 weeks of culture, we confirmed the cellular surface expression of both FcεRI and c-kit (>95% positive).

Differentiation of iPS cells to mast cells

Before coculturing with OP9 cells or EB formation, mouse iPS cells were suspended in an ES cell medium and cultured on a culture dish at 37°C for 30 min to remove MEF layers. In the OP9 cell-mediated differentiation method, iPS cells were transferred onto OP9 cells in 6-well plates at a density of 1×10^4 cells per well. The induced cells were trypsinized on day 7, and 1×10^5 cells were seeded onto fresh OP9 cells with α-MEM supplemented with 20% FBS, 2 mM L-glutamine, 1×NEAA, 30 ng/mL IL-3, and 100 ng/mL SCF (Peprotech). After 7 days, nonadherent cells were reseeded onto fresh OP9 cells. The cells were subcultured every 7 days. We harvested the differentiated cells on day 28 and used them for further analysis.

In the EB-mediated differentiation method, iPS cell-derived EBs were generated by culturing iPS cells on a round-bottom low-cell-binding 96-well plate at 1×10^3 cells per well. iPS cell-derived EBs were collected on day 7, and were transferred to a Petri dish with Differentiation Medium I [Dulbecco's modified Eagle's medium containing 15% FBS, 1×NEAA, 2 mM L-glutamine, 1×nucleosides, 0.1 mM 2-mercaptoethanol, penicillin/streptomycin, 30 ng/mL IL-3, 30 ng/mL IL-6 (Peprotech), and 100 ng/mL SCF]. After 7 days, nonadherent cells were transferred to a culture dish with Differentiation Medium II (Dulbecco's modified Eagle's medium containing 10% FBS, 1×NEAA, 2 mM L-glutamine, penicillin/streptomycin, 30 ng/mL IL-3, and 100 ng/mL SCF). We harvested the nonadherent cells on day 28 and used them for further analysis.

Transmission electron microscopy

BMMCs or iPSMCs were fixed with 2.5% glutaraldehyde in 0.1 M sodium phosphate buffer (pH 7.4), postfixed with 1% OsO_4, dehydrated by a graded ethanol series, passed through QY-1 (Nisshin EM), and then embedded in Epon-812 (TAAB,). Ultrathin sections (0.06-μm thick) were cut with an ultramicrotome (Leica Microsystems), stained with uranyl acetate–lead citrate, and observed using an electron microscope (H-7650, HITACHI) at 80 kV.

Protease assay

BMMCs or iPSMCs were washed with phosphate-buffered saline (PBS), lysed in PBS containing 2 M NaCl/0.5% Triton X-100, and incubated for 30 min on ice. The lysate was centrifuged at 12,000 rpm for 30 min at 4°C. Activities of granule proteases in the resultant supernatants were measured using their specific chromogenic peptide substrates, such as S-2288 for tryptase (Sekisui medical) and M-2245 for carboxypeptidase A (CPA; Bachem) [24].

β-hexosaminidase release assay

β-hexosaminidase activity was measured as a marker of the granular fraction for evaluation of degranulation. Cells were washed with an HEPES buffer (137 mM NaCl, 20 mM HEPES, 5 mM D-glucose, 2.7 mM KCl, 0.4 mM NaH_2PO_4, 0.5 mM $MgCl_2$, 2.4 mM $CaCl_2$, and 0.1% bovine serum albumin) and incubated with the buffer containing compound 48/80 (10 μg/mL; Sigma) or substance P (100 μM; Sigma) for 30 min. In the case of antigen stimulation, mast cells sensitized with 1 μg/mL anti-dinitrophenyl (DNP) IgE (SPE7; Sigma-Aldrich) for 24 h were stimulated with 100 ng/mL DNP-human serum albumin (HSA; Biosearch Technologies) in the presence of lysophosphatidylserine (Lyso-PS; Avanti Polar Lipids).

Coculture of mast cells with Swiss 3T3 fibroblasts

iPSMCs obtained after 28 days of culture with OP9 cells were cocultured with mitomycin C-treated Swiss 3T3 fibroblasts in the presence of 100 ng/mL SCF. BMMCs were

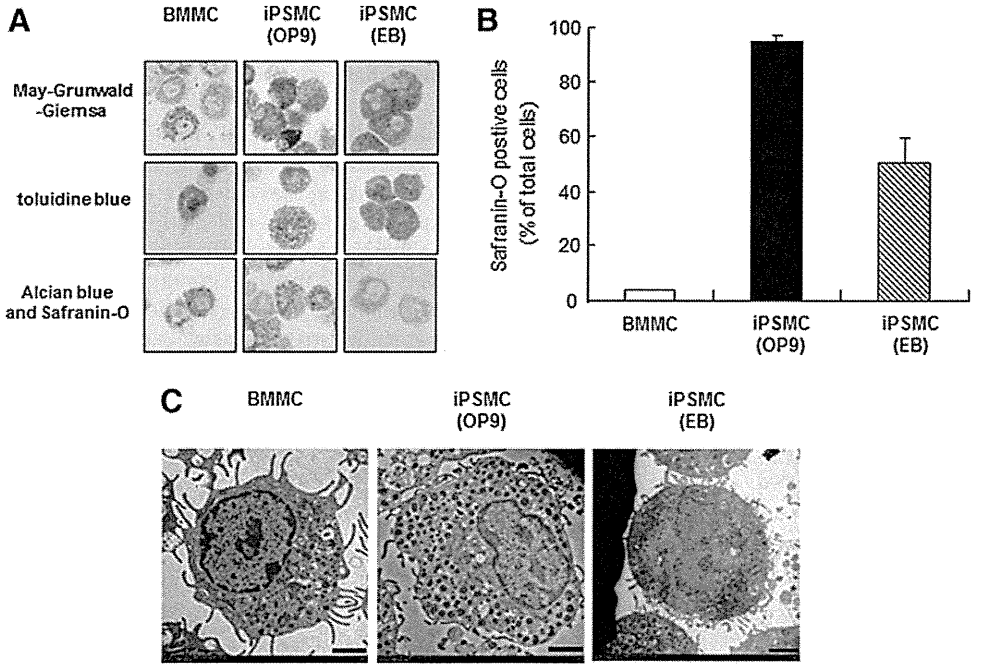

FIG. 1. Morphological characterization of induced pluripotent stem cell-derived mast cells (iPSMCs). **(A)** The iPSMCs, which were differentiated by coculture with OP9 cells or the embryoid body formation method, were harvested on day 28. Cytocentrifuged preparations of bone marrow-derived mast cells (BMMCs) and the iPSMCs were stained with May-Grunwald-Giemsa, toluidine blue, or Alcian blue and Safranin O solutions. **(B)** The ratio of Safranin O-positive cells to total cells was calculated and shown as a percentage. The data represent the means ± S.D. ($n=4$). **(C)** BMMCs and iPSMCs were visualized by transmission electron microscopy. Scale bar = 2.0 μm.

also cocultured with Swiss 3T3 fibroblasts under the same conditions. The subculture was performed every 4 days. The cells were trypsinized and replated, and nonadherent cells were collected as mast cells and used for further analysis.

Mast cell reconstitution and induction of passive cutaneous anaphylaxis

BMMCs or iPSMCs (5×10^5 cells) were injected subcutaneously into the conjunctivae of mast cell-deficient $Kit^{W\text{-}sh/W\text{-}sh}$

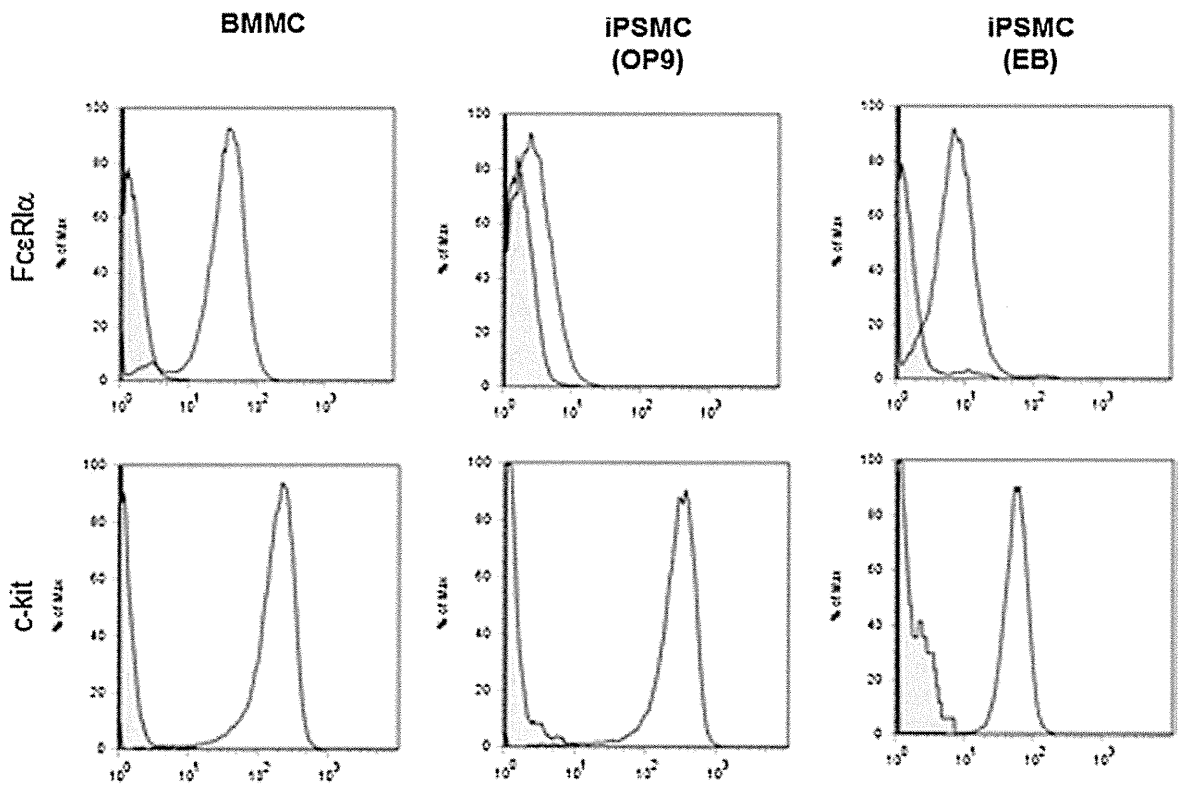

FIG. 2. Flow cytometric analysis of FcεRI and c-kit expression on iPSMCs. BMMCs and iPSMCs were stained with FITC-labeled anti-FcεRI and PE-labeled anti-c-kit antibodies for 30 min on ice. Stained cells were washed, resuspended in 1% fetal bovine serum–phosphate-buffered saline (FBS-PBS), and analyzed by flow cytometry.

mice. To elicit passive cutaneous anaphylaxis reactions, mice were injected subcutaneously into the conjunctiva with 75 ng anti-DNP IgE or saline. Then, 24 h after IgE injection, 100 μg DNP-HSA containing 2% Evan's blue dye was injected intravenously into mice. Thirty minutes later, the mice were killed, and their conjunctivae were excised. Evan's blue dye was extracted from conjunctivae with formamide, and the absorbance was measured at 610 nm.

Results

Generation of mast cells from mouse iPS cells

iPSMCs were generated by the OP9 coculture method or EB formation method as described in Supplementary Fig. S1 (Supplementary Data are available online at www.liebertpub.com/scd). Approximately 6.5×10^6 mast cells could be obtained from 1×10^5 iPS cells by coculturing them with OP9 cells for 4 weeks. In addition, as in the case of BMMCs, iPSMCs can retain their proliferative potential (data not shown).

Next, we performed the staining with May-Grunwald-Giemsa, toluidine blue, Alcian blue, and Safranin O solutions. May-Grunwald-Giemsa staining of the iPSMCs, which were differentiated by coculture with OP9 stromal cells or the EB formation method (Supplementary Fig. S1), revealed that induced mast cells gave rise to a uniform phenotype with rough basophilic granule-containing cells (Fig. 1A, upper). The granules in these cells showed a metachromatic staining pattern when stained with acid toluidine blue (Fig. 1A, middle). We then performed Alcian blue and Safranin O staining, by which mast cells are known to show a specific red color if they are CTMCs and a blue color if they are immature mast cells or MMCs [1]. While BMMCs were Alcian blue positive and Safranin O negative, iPSMCs were positive for both Alcian blue and Safranin O staining (Fig. 1A, [lower], B). Electron microscopic analysis revealed that the iPSMCs differentiated by either method contained more granules than BMMCs (Fig. 1C).

Expression of high-affinity IgE receptor on iPSMCs

Mast cells are known to express c-kit and FcεRI (high-affinity IgE receptor) [1]. We next performed flow cytometric analysis to examine the surface expression of c-kit and FcεRI on iPSMCs. There was no significant difference in c-kit expression levels between iPSMCs and BMMCs (Fig. 2). In contrast, the FcεRIα expression level was significantly lower in the iPSMCs that were generated by coculture with OP9 cells, compared with that in BMMCs. Both c-kit$^+$FcεRI$^+$ and c-kit$^+$FcεRI$^-$ cells showed a granular phenotype by forward and side scatter (data not shown).

FcεRI is a heterotrimer composed of one α-chain and 2 γ-chains or a heterotetramer composed of one β-chain and 2 γ-chains. To evaluate the expression of each FcεRI subunit in iPSMCs, we analyzed mRNA expression levels by reverse transcription and quantitative polymerase chain reaction (RT-PCR). As shown in Supplementary Fig. S2, the expression levels of the mRNAs encoding the FcεRIα, FcεRIβ, and FcεRIγ chains were reduced in the iPSMCs differentiated by either method as compared with the levels in BMMCs.

Phenotypic differences between iPSMCs and BMMCs

To further compare the degree of mast cell differentiation, we measured the tryptase and CPA activities in iPSMCs. The tryptase and CPA activities were elevated in the iPSMCs derived from either method as compared with those in BMMCs (Fig. 3).

Histidine decarboxylase (HDC) is a critical enzyme that is involved in the synthesis of endogenous histamine in mammals [25–26], and is considered to be one of the indices of mast cell maturation [26]. Therefore, quantitative RT-PCR analysis was performed to compare the expression of HDC mRNA levels in iPSMCs and BMMCs (Supplementary Fig. S3). The expression level of HDC mRNA was elevated in the iPSMCs that were differentiated by either method as compared with that in BMMCs.

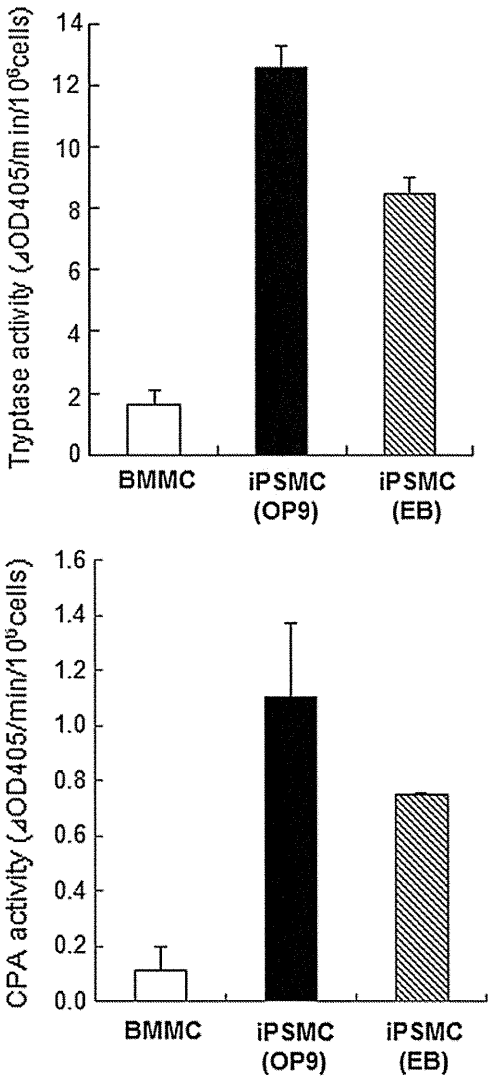

FIG. 3. Tryptase and carboxypeptidase A (CPA) activities in iPSMCs. Cell extracts prepared from BMMCs and iPSMCs were assayed for tryptase and CPA activities as described in the Materials and Methods section. All data represent the means ± S.D. ($n=4$).